University of Amsterdam
Van der Waals - Zeeman Institute

Bachelors Thesis in Physics

Light from Silicon Nanocrystals

Author:
Kasper van der Vaart

Supervisors:
W.D.A.M. de Boer
T. Gregorkiewicz

8th June 2009

Abstract

Silicon is the most used semiconductor in electronic industry. However, because of its indirect bandgap, which results in low light emitting efficiency, silicon photonic- & electro-optical devices have low efficiency. Silicon nanocrystals (Si NCs) offer a solution because of their tunable indirect bandgap. In this bachelor thesis photoluminescence (PL) measurements on Si NCs embedded in a SiO_2 matrix are reported. It is shown that a debated fast component (ns) in the PL decay, referred to as the F-band, has a red shift for smaller NCs. This F-band is ascribed to a direct bandgap recombination. Therefore it is found that due to quantum confinement the direct bandgap decreases. In combination with the phonon bottleneck effect, which slows down carrier cooling by phonon emission and therefore increases the probability of direct recombination for smaller NCs, this tunable direct bandgap offers new possibilities for efficient and tunable light emission of Si NCs.

Contents

1 Introduction **2**
1.1 Material and optical properties . . . 2
1.1.1 Silicon . . . 2
1.1.2 Silicon nanocrystals . . . 3
1.1.3 Photoluminescence . . . 4
1.2 Bandgap recombinations . . . 5
1.2.1 Fast and slow band . . . 5
1.2.2 Direct recombination . . . 7
1.3 Motivation . . . 9

2 Experimental methods **10**
2.1 Samples . . . 10
2.2 Photoluminescence spectra . . . 12
2.3 Photoluminescence kinetics . . . 13
2.4 Performing measurements and data processing . . . 13

3 Results **14**
3.1 PL spectra measurements . . . 14
3.2 PL kinetics measurements . . . 16
3.2.1 PL kinetics of the F-band . . . 17
3.3 Discussion . . . 20
3.4 Conclusions . . . 21

4 Outlook **22**

References **23**

A Nederlandse samenvatting **24**

Chapter 1

Introduction

1.1 Material and optical properties

1.1.1 Silicon

The most common semiconductor on earth and the most used in industry is silicon (Si). Si applications in the modern world are numerous. Ranging from glass, concrete, semiconductor devices (like solar cells and microchips) to synthetic plastic substances. The strength of Si lies in its abundance and its electrical properties which can be easily changed via doping. Condensed matter behaves either as an insulator, a conductor or a semiconductor. This behavior all depends on the particular energy band structure of the material. The band structure tells us at what energy levels electrons can exist. Si is a semiconductor, meaning it will only behave as a conductor when enough energy is added and the electrons can move from the valence band, across an energy gap, into a higher state in the conduction band. As the name implies, the electrons in the conduction band will enable conduction. In Si the energy gap between the valence and conduction band is indirect. Which means that the top of the valence band is shifted in **k**-space relative to the absolute minimum of the conduction band (Fig. 1.1).

When an electron is excited into the conduction band it will leave a hole in the valence band. There are numerous ways for the electron to lose its energy and recombine with a hole. An important distinction can be made between radiative and non-radiative recombination. The former process involves losing energy by emitting a photon, the latter (of which there are different forms) does not involve photon emission. In the case of radiative recombination, an electron high in the conduction band will lose energy by emitting phonons and move down to the bottom of the conduction band. In the case of a direct bandgap the electron-hole pair will recombine and emit a photon with an energy corresponding to the bandgap. While in the case of the indirect bandgap of Si, the electron and hole will only recombine radiatively when in addition to the energy difference also the momentum difference can be compensated. Hence, together with the emitted photon, a phonon must be emitted or absorbed. Such a phonon-photon combination is far less likely to occur than other non-radiative recombinations in Si. This results in inefficient optical activity [1, 2]

and very much limits the advancement in Si photonic applications.

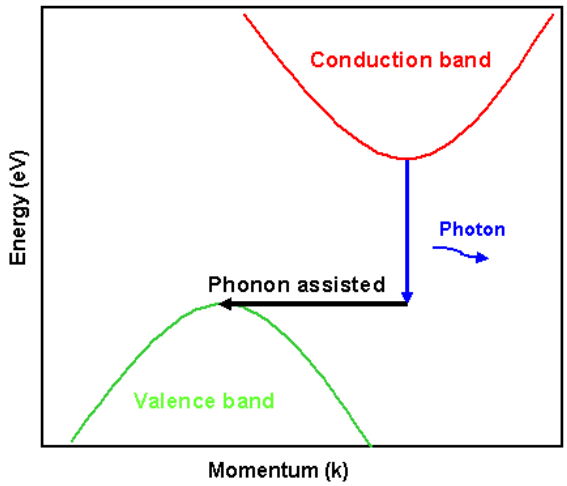

Figure 1.1: Indirect bandgap

1.1.2 Silicon nanocrystals

A way to improve the optical activity of Si is by forming it into nanocrystals (NCs), also called quantum dots. NCs range in size from 1 to 100 nm and consist of hundreds to millions of atoms. The energy structure of a NC resembles to a certain extent that of a single atom, hence they are often called artificial atoms. An atom has distinct energy states. Whereas bulk material has a band structure. When the dimensions of an atomic structure become comparable to the Bohr radius of an exciton, the band structure is changed. This effect is referred to as quantum confinement [3]. Quantum confinement splits the energy bands into quantized states. In addition, when the NC size decreases, the conduction band moves up and the valence band moves down, thereby increasing the bandgap energy value. Moreover, according to Heisenberg's uncertainty principle $\Delta x \Delta p \geq \frac{\hbar}{2\pi}$, if the position of an electron is better defined (as is the case of a NC) the uncertainty in momentum will increase. Recombination will then happen "pseudo" direct, without phonons. Hence, making it more probable for an electron to recombine radiatively. This is known as relaxation of the momentum conservation rule. One more important phenomenon, predicted theoretically, although not yet experimentally proven, occurs in NCs. Namely, due to quantization of the energy bands, the probability for an electron to cool down from a high state to the bottom of the conduction band by emitting phonons decreases. This is known as the phonon bottleneck [4]. As a consequence, the efficiency of radiative recombination increases.

1.1.3 Photoluminescence

The process of emitting a photon after excitation is called photoluminescence (PL). The emitted wavelength depends on the energy level of which the electron-hole recombination takes place. When a sample with Si NCs is excited and the detected intensity is plotted as a function of wavelength, a PL spectrum is recorded (Fig. 1.2(A)). In case of a A PL spectrum can be plotted as a function of energy. Wavelength λ (nm) can be converted to energy (eV) using

$$E = \frac{hc}{\lambda} \approx \frac{1240}{\lambda}, \tag{1.1}$$

where h (eV s) is Planck's constant and c (nm/s) the speed of light. In case of a simple transition in a 2-level system, a PL spectrum has a Gaussian shape, caused by the size distribution of the NCs. A narrow peak indicates a small size distribution. However, if there are more energy states present the shape of the PL spectrum depends on the corresponding transitions. In case of pulsed excitation, a PL spectrum is taken for a predetermined time window, collecting all the photons emitted within that window and integrating time. Different time windows will result in different spectra. When excitation is done with a continuous wave laser the Si NCs reach an equilibrium of excitation and recombination. A spectrum that is taken over the full emission time of a sample which is in equilibrium, is called a Steady State PL (SSPL) spectrum.

As mentioned above there are radiative and non-radiative processes in NCs, on which the effective PL life time depends. The for Si NCs important Auger non-radiative processes depend on the number of electrons in the conduction band and are faster than radiative processes. Since free electrons have short lifetimes, at short time scales the dominant contribution to the PL are non-radiative processes and at longer time scales radiative processes. To monitor both, PL can be detected in a time-resolved way (Fig. 1.2(B)). This is referred to as PL kinetics. From the PL kinetics an effective decay time can be estimated.

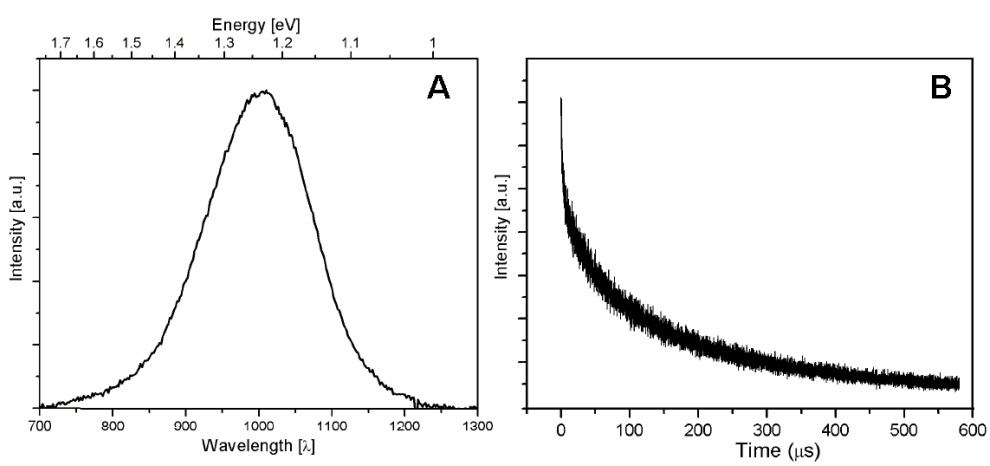

Figure 1.2: (A) PL spectrum. (B) PL kinetics.

1.2 Bandgap recombinations

1.2.1 Fast and slow band

The PL emission of Si NCs has been studied intensively. But some findings prove difficult to understand and are still under debate. Research shows two different features in the PL. Namely, for small NCs (3 nm) the PL spectra moves to shorter wavelengths (higher energy) and the intensity increases as described in Section 1.1.3. This emission is referred to as the "slow" PL or "slow" band (S-band) because it has a decay time ranging from micro- to milliseconds. In addition to the S-band, another emission occurs at even shorter wavelengths with a much faster decay time ranging from nano- to picoseconds. This emission is called the "fast" PL or "fast" band (F-band). The S-band's origin is acknowledged to be recombination from the lowest possible energy state. In Si NCs smaller than 3 nm, recombination can also occur from a trapping state on the NC surface, which forms an inter-bandgap energy level [5]. However, the mechanism causing the F-band is debated. One interpretation is reported in Ref. [6]. It is stated that a "fast" PL decay component, although not identified as the F-band, is the result of recombination from the NC core and a slow component arises from recombination from a trapping state on the NC surface. In Fig. 1.3 the recombination mechanism from Ref. [6] for Si NCs is shown.

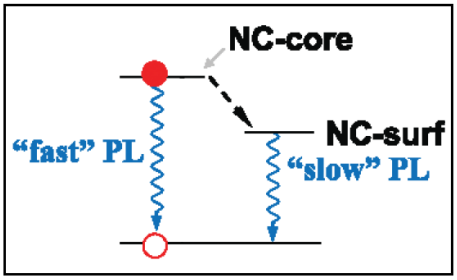

Figure 1.3: The mechanism for the "fast" PL and "slow" PL from Ref. [6].

To support this model the authors present a number of figures. Of which the most important are shown in Fig. 1.4. The main points in Ref. [6] are the characteristics of the two different PL phenomena - "fast" PL & "slow" PL - and how they are related to two different recombination mechanisms. The measurements indicate that the "fast" PL is size dependent and the "slow" PL is not. Hence, the model which states that the "slow" PL is caused by the NC surface state recombination and the "fast" PL by the NC core itself.

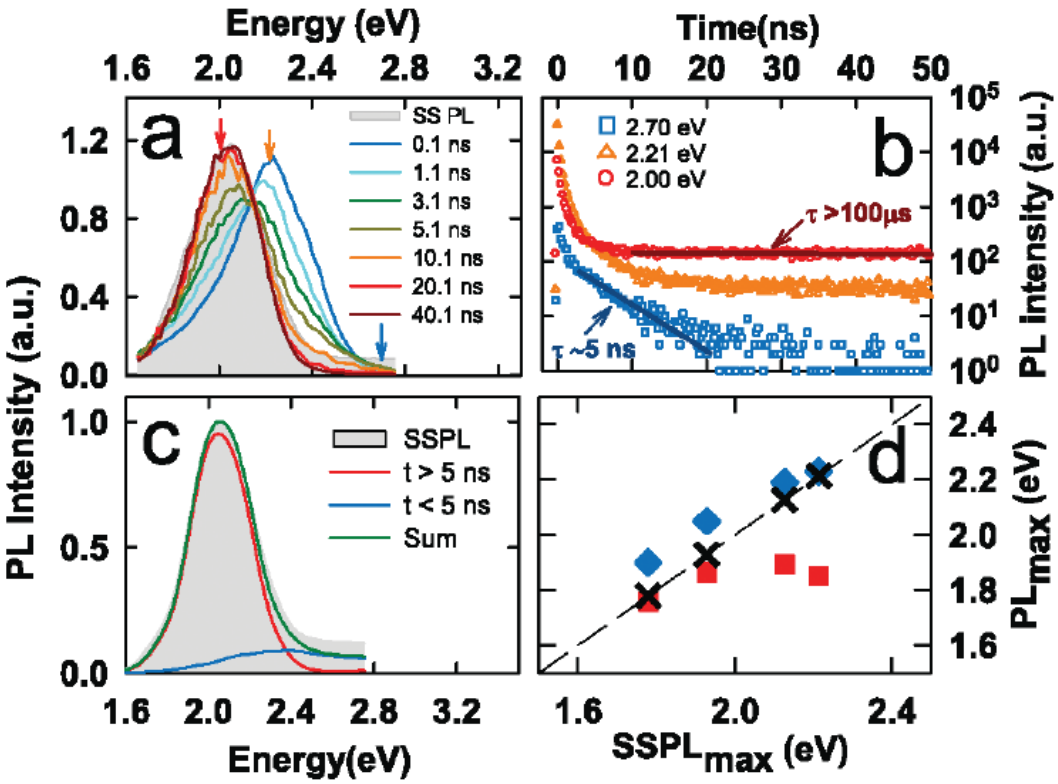

Figure 1.4: Figures from Ref. [6]. (a) Changing of the PL spectrum in time. Spectra are normalized to the same area. The SSPL is taken at $t > 100$ μs. (b) PL kinetics for the energies marked in (a). (c) PL spectra generated by time integrating PL kinetics for different wavelengths. (d) The dependence of the "fast" PL (blue) and the "slow" PL (red) peak energy on the SSPL peak energy ($\times$).

Here follows a short discussion on the figures presented in Ref. [6]. In Fig. 1.4(a) PL spectra are shown at different times. It can be seen that after the first ns the PL peak is at its highest energy. After that it starts to decrease in energy until around 3 ns it overlaps with the SSPL. The increase and decrease in intensity is caused by the normalization. The authors conclude from this picture that there are two distinct PL emission components at different energies. The higher energy component is stronger within the first ns and after 3 ns the lower energy PL takes over. In Fig. 1.4(b) PL kinetics are shown taken at energies indicated by the arrows in Fig. 1.4(a). For the highest energy (2.70 eV) the decay is fast, with a decay time of 5 ns. For the lower energies there is a long decay time ($\tau > 100\mu s$). In Fig. 1.4(c) PL kinetics for different wavelengths have been time-integrated resulting in three PL spectra for different time windows. The fast component from Fig. 1.4(b) indeed originates from higher energies (blue line). This is in agreement with Fig. 1.4(a). The slow component (red line), originates from lower energies. The sum of both PL (taken over the entire time window) overlaps closely with the SSPL (gray shading). According to Fig. 1.4(d) the peak energy of the higher energy fast component follows the SSPL peak. However, the

peak energy of the lower energy slow component does not show this. Considering that the SSPL peak changes with NC size, the authors conclude that the low energy slow component is size independent and the high energy fast component is size dependent. Hence the fast component must be caused by the NC core and the slow component by external NC surface states. The model from Ref. [6] is but one interpretation of the PL phenomena of Si NCs. In the next section a different one is discussed.

1.2.2 Direct recombination

In February 2009 a new mechanism was proposed for the origin of the F- and S-band [7]. Theoretical research showed that in addition to the increase of the indirect bandgap due to quantum confinement, the direct bandgap decreases in the Γ_{15} point. This can be seen in Fig. 1.5, which shows the bandgap structure of Si. As described in Section 1.1.2, quantum confinement causes the $\Gamma_{25'}$-point to move down and the Δ_1 valley bottom to move up, thus increasing the indirect bandgap. However, in Ref. [7] is shown that the Γ_{15}-point also moves down but faster than the $\Gamma_{25'}$-point, making the direct bandgap smaller. Combined with the phonon bottleneck, which decreases the cooling probability of electrons to the Δ_1 valley, this results in an increasingly efficient tuneable direct bandgap transition for smaller NCs.

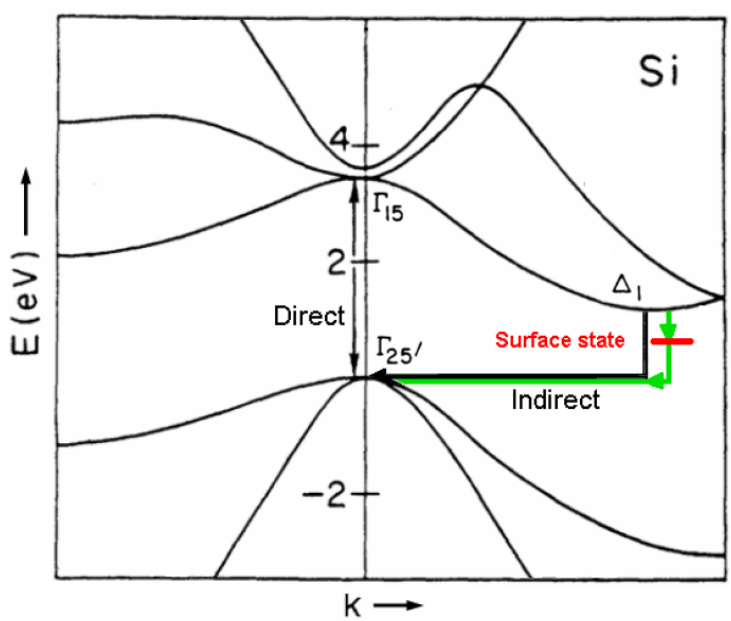

Figure 1.5: The bandgap structure of Si with the indirect and direct electron-hole recombinations. An indication of the NC surface state (red) and recombination via the surface state (green) [9].

According to Ref. [7] it is the direct bandgap recombination that is responsible for the F-band. The S-band arises due to a recombination from the indirect bandgap and surface states. Presumably the emission of these closely overlap in energy [8]. Therefore usually a combination of these two recombinations is observed. Fig. 1.6 shows the theoretical calculation of the change in bandgap energy value as a function of NC size. According to these calculations the F-band would decrease in energy for smaller NCs. The S-band's energy will increase for smaller NCs, which is in agreement with the above mentioned quantum confinement behavior. Fig. 1.6 also shows experimental results for both the F- and S-band, which confirm the depicted model. The data points were obtained using a different PL setup from the one used for this report, except for the lowest point, which could not be measured with that setup and will be shown in Section 3.2.1. The different F-band energy lines in Fig. 1.6 represent different transitions between electron and hole quantized levels.

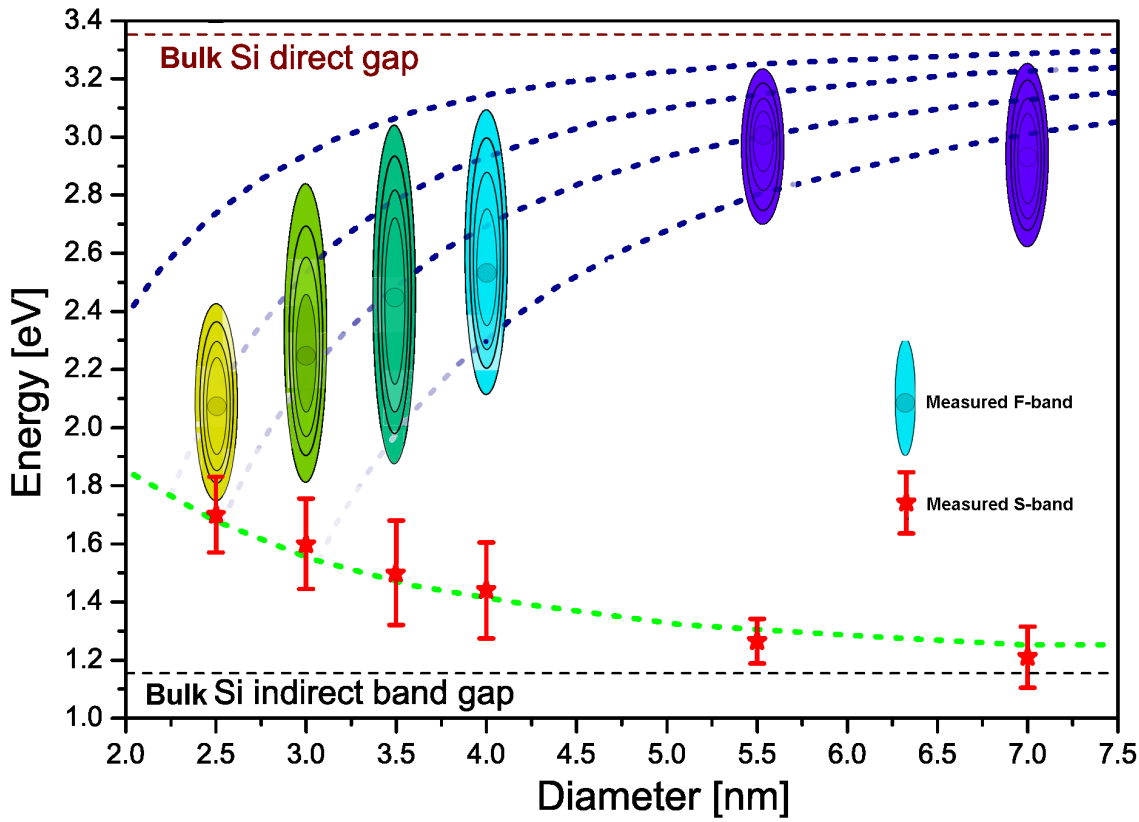

Figure 1.6: Theoretical F-band energy value (blue dotted lines) and S-band energy value (green dotted line) as a function of NC size. Experimental results for the F-band (colored dots) and S-band (red stars) obtained in a different setup from the one used for this report, except for the lowest F-band point. Bulk Si direct bandgap energy (brown dotted line) and indirect bandgap (black dotted lines).

1.3 Motivation

Light is used as an energy source through solar cells. Considering the depletion of the earth's mineral resources there seems no other option but to go the hard way and make a complete switch to solar energy. Because of the tunable indirect bandgap of Si NCs, a lot of effort is already made to implement Si NCs in solar cells. Now the tunability of the direct bandgap in combination with a higher probable direct recombination because of the phonon bottleneck, is a major discovery which could open the way for higher efficiency solar cells. Higher efficiency solar cells generate more energy and can therefore be made thinner, which in addition reduces cost. This a major motivation for research on optical and material properties of Si NCs.

Chapter 2

Experimental methods

For this report PL measurements were used to characterize Si NC samples. Time-integrated and time-resolved PL measurements were performed at room temperature to determine the mean size of the Si NC samples, decay times and spectral characteristics of the F- and S-band. The experimental methods, setup and preparation of the samples will be discussed below.

2.1 Samples

The samples are composed of a 2 μm layer of Si NCs embedded in SiO_2 on a SiO_2 substrate. Production was done with the sputtering method. In Fig. 2.1 the mechanism for sputtering is shown. A voltage is applied between the magnetron sputtering cathode and the anode, which is located above the substrate. A gas is injected between the substrate and the cathode. The gas will be ionized by the electric field. The lower magnets trap the gas near the target material, which in this case are Si and SiO_2. When the gas ions collide with the target, Si and SiO_2 will be ejected onto the substrate [10]. After sputtering there are scattered Si atoms among the SiO_2 molecules on the surface of the substrate and not yet any NCs. To "grow" the Si NCs the sample is heated for 30 minutes at around 1100 °C. The effect of heating lets the Si atoms cluster into crystals. This will result in a distribution of different sized NCs with a mean size dependent on the heating temperature and amount of Si material used. The size distribution of the NC samples used in this report is 14% [11]. In Fig. 2.2 mean NC size is plotted as a function of S-band PL peak energy. Using Formula 1.1 the peak energy can be related to emission wavelength.

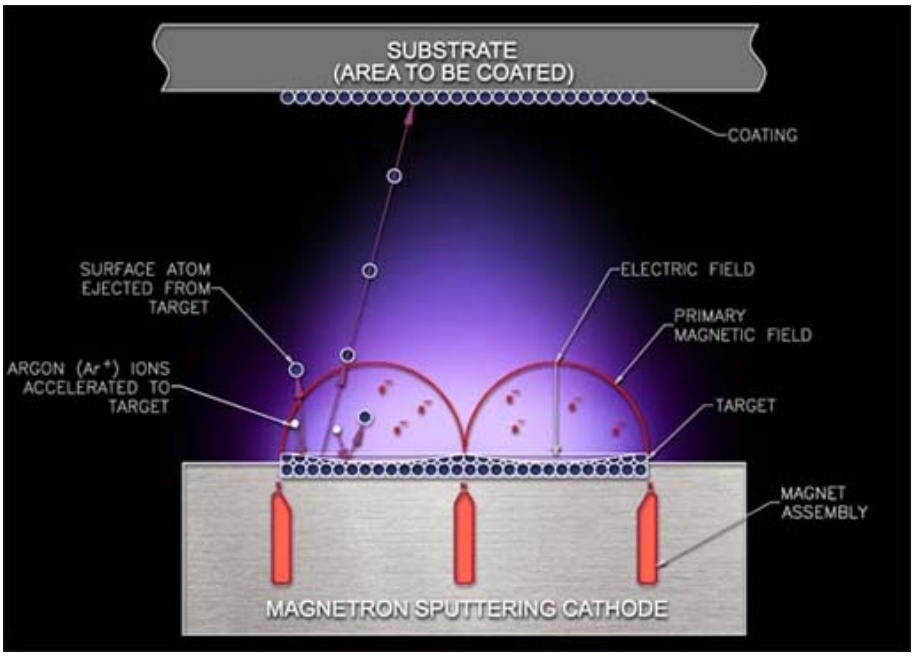

Figure 2.1: The sputtering mechanism shown in Ref. [10].

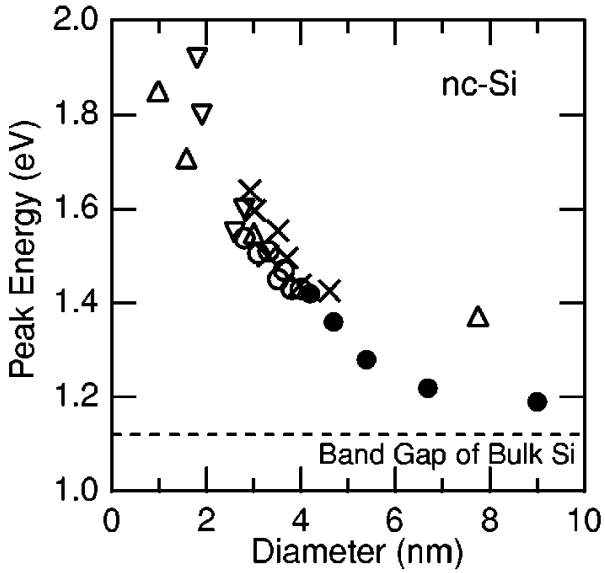

Figure 2.2: PL peak energy versus average diameter of Si NCs. The size is measured with cross-sectional transmission electron microscopy [11].

2.2 Photoluminescence spectra

By directing a laser beam with the correct wavelength on a sample, electrons will be excited and the NCs will emit. The 3rd harmonic of a pulsed Nd:YAG laser is used, with a wavelength of 355 nm, pulse duration of 5 ns and a repetition rate of 20 Hz. PL spectra are measured with the setup shown in Fig. 2.3. To change the wavelength of the laser an Optical Parametric Oscillator (OPO) is used. The OPO has a nonlinear crystal which splits the photons in the incoming laser beam in two. One in the visible range and one in the infrared. For this report only the visible one is used, therefore the other one is blocked by a band-pass filter. By changing the angle of incidence of the laser beam with respect to the nonlinear crystal, the OPO can generate wavelengths between 420 and 2250 nm. The OPO beam is then directed and focussed on the sample via a number of mirrors and lenses. To adjust the power of the beam two polarizing filters ar used. The light emitted from the sample is focussed by two lenses and enters a Jobin-Yvon TRIAX 320 monochromator. A filter is placed in front of the monochromator to block scattered or reflected laser light. Because the detector itself cannot distinguish wavelengths (it only counts photons), the monochromator picks out a desired wavelength from the incoming light. The detector used is a Hamamatsu R5509-72 near-IR photomultiplier tube (PMT). The PMT is connected to a digital scope which is used to show the signal of the detector. A photodiode is connected to the scope for triggering. A computer is connected to the scope and integrates the signal over the full time decay of the PL. For comparison, spectra have also been taken with a different detector, namely an Edinburgh Instruments Germanium EI-A detector.

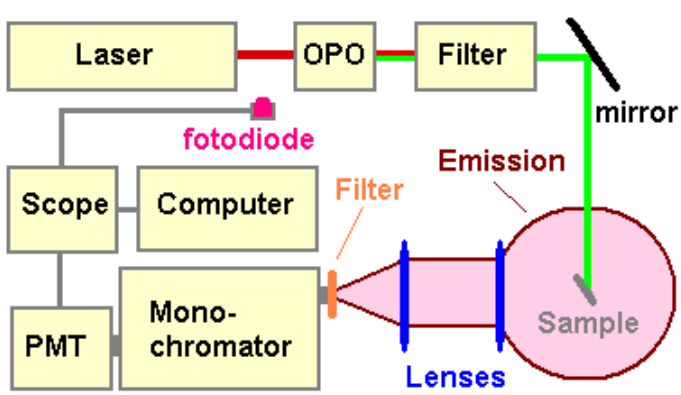

Figure 2.3: The setup used for PL measurements.

2.3 Photoluminescence kinetics

To monitor PL kinetics the same setup is used in a photon counting configuration. The computer uses a photon-counting system card which registers individual detected photons in digital "bins" of a predetermined time window. An integer output is then obtained. All bins together form the entire time window. The smallest bin-size of "1" corresponds with 0.25 ns. A bin-size of 128 then corresponds with 32 ns. The bin-range sets the amount of bins for the entire time window. For instance with a bin-size of 128 and a bin-range of 1000, the time window is 32 μs. The PMT has a time-resolution of 1.3 ns. Hence, kinetics can be measured up to the ns region. After measuring, the data must be fit with an exponential decay function to estimate the decay time constant. A normal exponential function does not fit with Gaussian size distributed NCs. Hence, a stretched exponential is used, with $\Phi(t)$ the intensity at time t, I_0 the intensity at $t = 0$, τ the decay time constant and $\beta = 0.8$ in the case of a Gaussian distribution [12]:

$$\Phi(t) = I_0 e^{-(t/\tau)^\beta}. \tag{2.1}$$

2.4 Performing measurements and data processing

Before measuring, the PMT must be cooled with liquid nitrogen for two hours. The temperature of the PMT is then -80 °C. The sample must be cleaned and positioned on a sample holder. The setup must be tuned for optimal signal. This is done by adjusting the OPO beam position on the sample, the sample's position, the position of the lenses towards the entrance of the monochromator, the laser intensity and the monochromator aperture. In this process the scope is used for optimization. The measurements results are collected in ASCII files with an integer intensity value for each wavelength. These files are then processed (Origin 7 or 8) to construct spectra or kinetics. No absolute intensity measurements were done, hence PL spectra had to be normalized. As mentioned above PL kinetics were fit using a stretched exponential.

Chapter 3

Results

For this report nine Si NC samples, with sizes ranging from 2.7 nm to 6.6 nm, were analyzed. Both SSPL spectra and PL kinetics were taken. For two samples with a size of ∼2.7 nm and ∼3.1 nm an F-band spectral profile is constructed using PL kinetics. The resulting two F-band's will be compared with Fig. 1.6. The 2.7 and 3.1 nm samples have also been used in Ref. [7], but for the latter the F-band could not be resolved there. However, it is measured for this report and shown in Fig. 1.6.

3.1 PL spectra measurements

To determine the mean size of the samples, PL spectra of the S-band were measured. Excitation was done at 500 nm and PL detection ranged from 600 to 1300 nm. The filter used in front of the monochromator blocked below 550 nm. Fig. 3.1 shows the PL spectra for the nine samples. The spectra are normalized and clearly have different peak wavelengths. The mean size has been determined using Fig. 2.2 and is shown in Table 3.1. The samples which have a peak at shorter wavelength have a smaller mean size. The sample names correspond to the amount of Si used for sputtering and the annealing temperature. For instance Si6T1100 implies that the annealing temperature was 1200 °C and that six a.u. of Si were used for sputtering. It can be seen that for samples with a larger amount of Si sputtered the NCs are larger, however sample Si10T1100 is an exception. The annealing temperature also seems to increase the size of NCs.

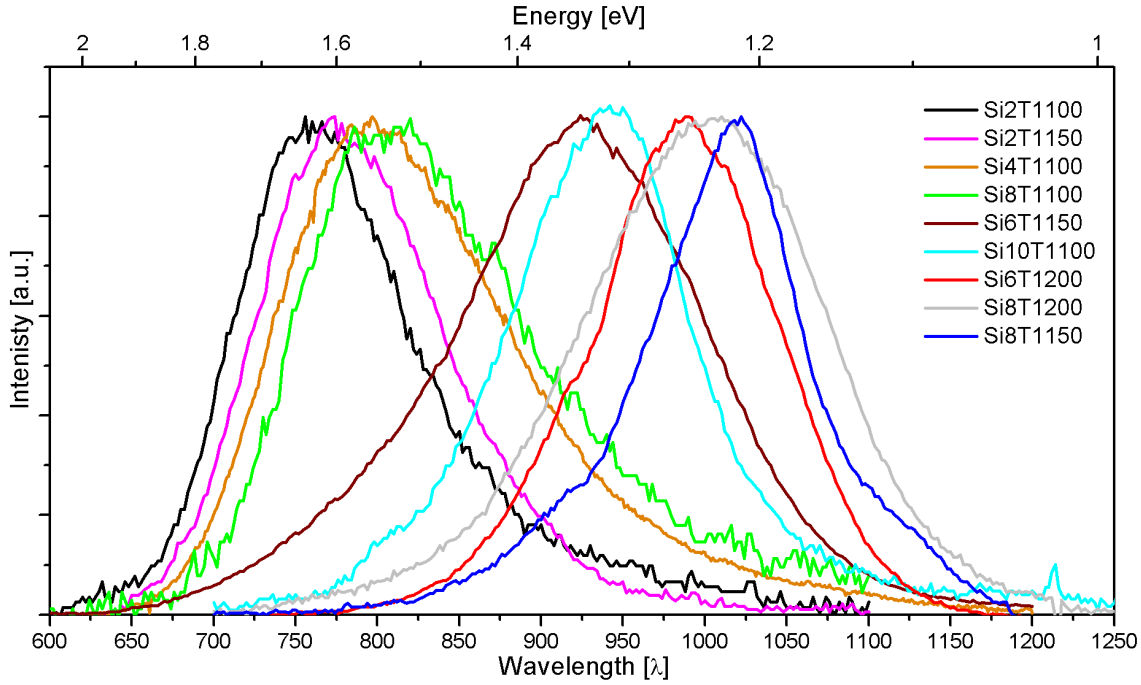

Figure 3.1: Normalized PL spectra of the Si NC samples.

Sample	PL peak (λ)	NC size (nm)
Si2T1100	760	2.7
Si2T1150	775	2.8
Si4T1100	800	3.1
Si8T1100	810	3.2
Si6T1150	920	4.6
Si10T1100	945	5.0
Si6T1200	990	5.9
Si8T1200	1000	6.1
Si8T1150	1020	6.6

Table 3.1: Mean sizes and corresponding PL peak wavelength of the Si NC samples.

3.2 PL kinetics measurements

For sample Si2T1100 and Si4T1100 PL kinetics were measured for two different time windows, namely 100 ns and 1 ms. Fig. 3.2(A) shows the PL kinetics for Si2T1100. The excitation wavelength is 500 nm and detection wavelength is the PL peak wavelength of the sample (Fig. 3.1). The decay time obtained from the stretched exponential fit is ∼25 μs. The PL kinetics for Si4T1100 in Fig. 3.2(B) show the same decay time. Considering the relaxation of momentum conservation (see Section 1.1.2) the decay of the smaller sample Si2T1100 should be faster than that of Si4T1100, however the kinetics do not clearly show this. The PL kinetics of Si2T1150 and Si8T1100, which are of the same size as Si2T1100 and Si4t1100 respectively show longer decay times. From Fig. 3.2(A) and (B) it is not immediately evident that, besides the μs decay, there is another decay process present. Therefore the PL kinetics in a time window of 100 ns were measured. The results will be discussed below.

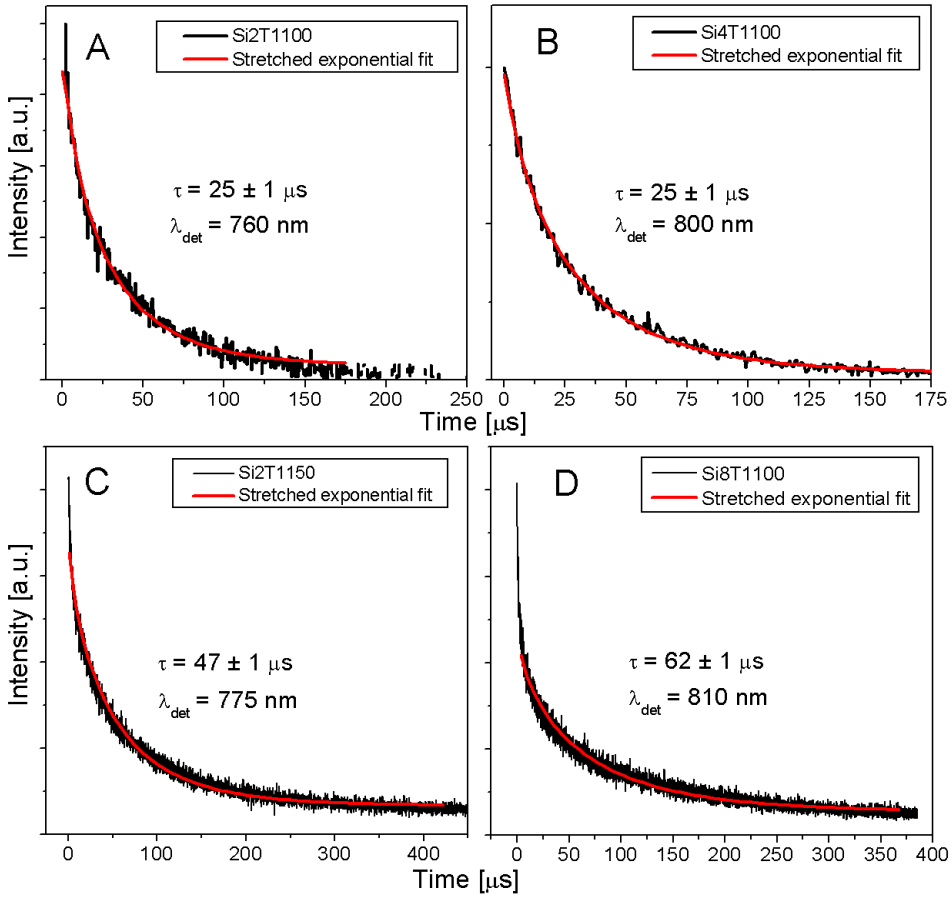

Figure 3.2: PL kinetics of sample Si2T1100, Si4T1100, Si2T1150 and Si8T1100. Red lines are stretched exponential fits with Formula 1.1. Estimated decay time constant and detection wavelength are given.

3.2.1 PL kinetics of the F-band

To determine the F-band, taking an SSPL spectrum is not a suitable method. The F-band will be obscured by the S-band's intensity because the S-band is the dominant contribution to the PL signal. However, when taking ns time-resolution PL kinetics the F-band's fast decay can be observed. It is then possible to construct a spectral profile from the amplitude of the F-band's decay component for different wavelengths. The F-band data points in Fig. 1.6 are obtained using this method with PL kinetics taken with a different setup. However, for Si2T1100 it was not possible to resolve the F-band. With the setup used for this report a fast decay component of ns could be observed for both Si2T1100 and Si4T1100. Considering the setup's time-resolution of 1.3 ns, this decay component cannot be conclusively established to be the decay of the F-band, which is in the order of 1 ns [7]. Nonetheless (with a bin-size of 0.25 ns) the amplitude of this fast decay component is indicative for the F-band's decay and can be used to construct a spectral profile.

Sample Si2T1100

To clearly show the fast decay component in the PL kinetics of Si2T1100, measurements were done in a time window of 100 ns with excitation wavelength of 420 nm. In the inset of Fig. 3.3 the result is shown for different detection wavelengths. The fast component appears around 5 to 15 ns, with a much higher intensity than the slow component at $t > 20$ ns. The fast component increases in intensity over the whole range of 900 to 650 nm, indicating that its peak intensity is not within the measured range. The slow component rises and increases from 900 till 750 nm and from 700 till 650 nm it decreases. The peak of this slow component should be around 760 nm according to the SSPL in Fig. 3.1. The spectral profile of the F-band is shown in Fig. 3.3 (blue line) with its peak wavelength at ∼580 nm. The SSPL of Si2T1100 is also plotted (black line). The shift between the F-band and SSPL indicates that the latter originates from a higher energy state. The same procedure as for the F-band was used to construct a spectral profile of the S-band. However, in this case the intensity of the slow component ($t > 20$ ns) was taken. The result is shown in Fig. 3.3 (red line).

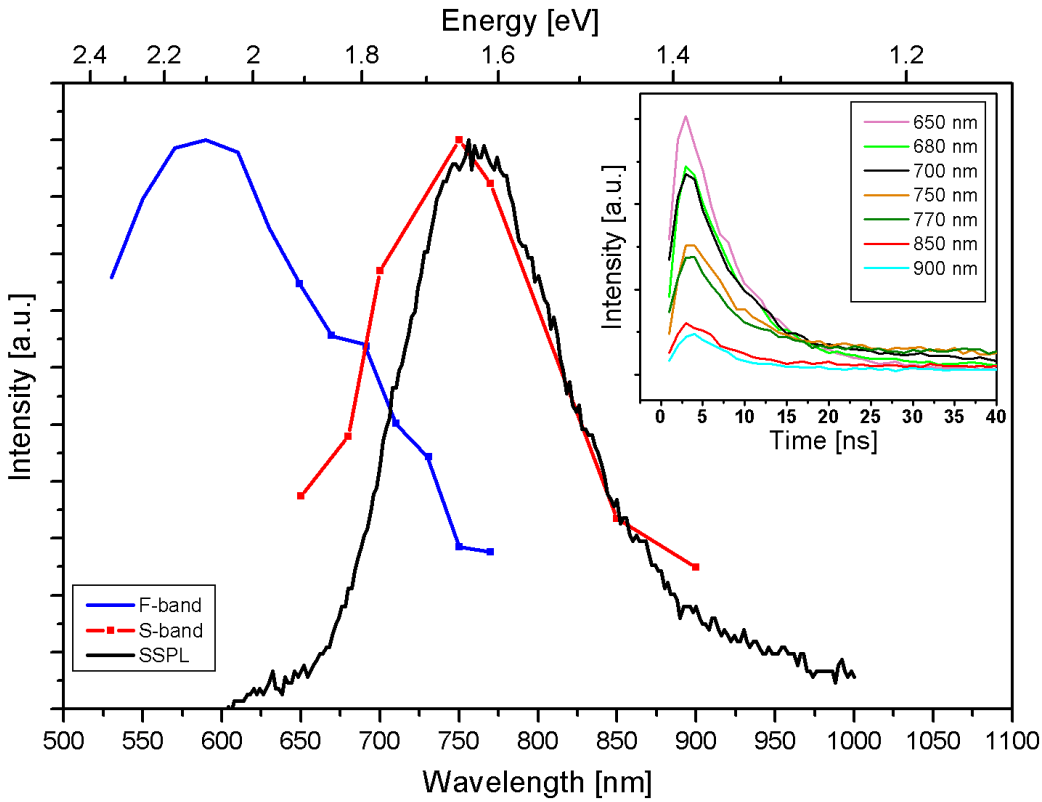

Figure 3.3: Normalized SSPL (black line), F-band (blue line) and S-band (red line) of Si2T1100. The inset shows PL kinetics of Si2T1100 for different detection wavelengths. Blue dots correspond with peak intensities obtained from the kinetics in the inset.

Sample Si4T1100

The same procedure was followed to measure the PL kinetics of Si4T1100 and construct a spectral profile. However, the excitation wavelength needed to be lowered to 355 nm. The reason for this will be discussed in Section 3.3. The measured PL kinetics of Si4T1100 are shown in the inset of Fig. 3.4. In Fig. 3.4 the F-band's spectral profile (red) is shown together with the SSPL (black). The F-band was corrected for the PMT's sensitivity and is also shown (blue). The decrease of the F-band near 400 nm is considered to be artificial for reasons that will be discussed below. It was not possible to construct a spectral profile for the S-band because the intensity of the tail of the kinetics is too low.

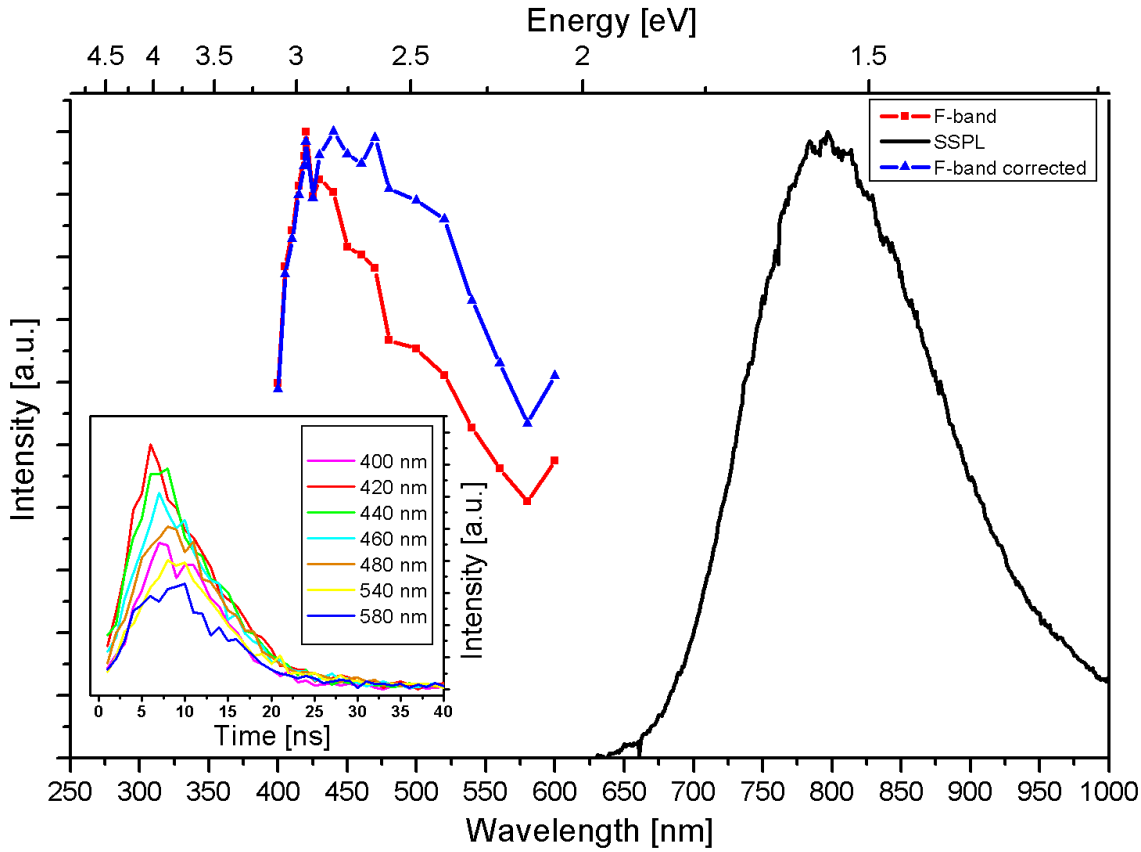

Figure 3.4: Normalized SSPL (black line), F-band (red line) and F-band corrected for PMT's sensitivity (blue line) of sample Si4t1100. Inset shows PL kinetics of Si4T1100 for different detection wavelengths.

3.3 Discussion

Here the results from previous sections will be discussed and compared with the model of direct and indirect recombination mechanisms (see Section 1.2). The SSPL measured shows normal S-band behavior for all samples. Namely, a shift in the PL peak wavelength toward higher energy for smaller NCs (Fig. 3.1). A larger PL peak energy originates from a larger bandgap transition. This corresponds to the indirect bandgap transition, which increases (according to quantum confinement) for smaller NCs (Fig. 1.6). In addition, the S-band's spectral profile of Si2T1100 constructed from the slow decay component of the PL kinetics, closely overlaps with the measured SSPL (Fig. 3.3). This is in agreement with Fig. 1.4(c).

The measured PL kinetics for a time window of μs do not show a clear sign of relaxation of the momentum conservation rule. The reason for this could be that the samples only differ in a range of $\sim$0.4 nm. Relaxation of the momentum conservation rule might be observed when comparing samples that differ more in size.

When measuring ns resolution kinetics of Si4T1100 the excitation wavelength needed to be lowered to 355 nm because of complications which arose when detecting close to the excitation wavelength. The excitation wavelength must differ as much as possible from detection wavelength and needs to be blocked by a filter. The filter used cuts the light at 380 nm. The decrease of the F-band near 400 nm (Fig. 3.4) is possibly caused by the filter. Therefore the measured peak wavelength of the F-band of Si4T1100 cannot be conclusively established to be at 425 nm. The peak wavelength of the F-band of Si2T1100 is around 580 nm (Fig. 3.3). From Formula 1.1 follows a bandgap energy of 2.1 eV. The peak wavelength of the F-band of Si4T1100 could not be determined. The F-band's spectral profile does not show a clear peak, considering that the decrease near 400 nm is artificial (Fig. 3.4). The F-band peak energy for NC size 3 nm from Fig. 1.6 is 550 nm. However, from Figs. 3.3 and 3.4 can be seen that for the smaller sample Si2T1100 the F-band's peak is at a longer wavelength compared to that of sample Si4T1100. In the case of energy this means that the F-band of the smaller sample Si2T1100 has a lower energy than that of the larger sample Si4T1100. This is in accordance with theoretical calculation in Fig. 1.6, showing that for smaller NCs the direct bandgap decreases.

The results acquired contradict the model shown in Fig. 1.3. If the F-band is caused by the indirect bandgap transition than according to Fig. 1.6 the bandgap energy should increase when going to smaller NCs. However, for the results shown here the opposite is the case. In addition, the overlap of the S-band's spectral profile with the SSPL (Fig. 3.3) shows that the S-band is not size independent as stated in Ref. [6], but has moved with the SSPL.

3.4 Conclusions

The obtained spectral profiles for sample Si2T1100 and Si4T1100 of size ∼2.7 and ∼3.1 nm respectively, show that the F-band decreases in energy for smaller NCs. Combined with the increase in energy of the S-band this implies that the F- and S-band move towards each other for smaller NCs. This corresponds with the theoretical calculation and experimental data from Ref. [7] (Fig. 1.6). The F-band of sample Si2T1100 which could not be resolved in Ref. [7] is resolved here, however a peak could not be conclusively established. It is shown that due to quantum confinement the F-band energy decreases, contrary to the indirect bandgap, which increases. In addition, the spectral profile of the S-band overlaps with the measured SSPL. Therefore, the S-band in Si NCs could be ascribed to "pseudo" direct recombination from the indirect bandgap, possibly via NC surface states. Considering the theoretical calculations for the direct bandgap recombination, the F-band could be ascribed to the direct recombination.

Chapter 4

Outlook

The new model, which ascribes the F-band in Si NCs to direct recombination and proposes a decrease in the direct bandgap for smaller NCs, can obtain a stronger foothold if more accurate measurements are done on different kind of samples. In literature experimental results differ when analyzing Si NCs, which are made with different methods. For more accurate measurements, new samples can be fabricated with better mono-disperse distributions. In addition, oxidation can be decreased to exclude recombination from surface states. The exact mean size of the samples can be determined for instance with TEM. The limitations of the setup used were a ns time resolution and a 400 nm detection limit. With ps resolution time-resolved measurements the F-band decay and spectrum can be monitored. The detection limit prevented further F-band study on Si4T1100. A problem, which arose when detecting PL kinetics, was that results where inconsistent when measuring over the course of a whole day. Moreover a very low PL signal hindered good PL measurements. If the setup, samples and experimental conditions are improved, a more definite conclusion could be made about the proposed model.

Bibliography

[1] J.R. Hook, H.E. Hall, *Solid State Physics.* WILEY, second edition (2006).

[2] E. Rosencher, B. Vinter. *Optoelectronics.* Cambridge University Press (2002).

[3] A. Alivisatos, Science **271**, 933 (1996).

[4] H. Benisty, C. Sotomayor-Torres, C. Weisbuch, Phys. Rev. B **44** 44 (1993).

[5] M. Wolkin, J. Jorne, P. Fauchet, G. Allan, and C. Delerue, Phys. Rev. Lett. **82**, 197 (1999).

[6] M. Sykora, *et al.*, Phys. Rev. Lett. **100**, 067401 (2008).

[7] W.D.A.M. de Boer *et al.*, Submitted to Phys. Rev. Lett. 27 Jan 2009.

[8] S. Godefroo, *et al.*, Nature Nanotechnology **3**, 174 - 178 (2008).

[9] P. Lautenschlager *et al.*, Phys. Rev. B, **36**, 4821 (1987).

[10] A.L. Wolf, *Investigation of CrSb as a possible half-metal.* Master thesis, University of Amsterdam (2005).

[11] S. Takeoka, M. Fujii, and Shinji Hayashi, Phys. Rev. B, **62**, 16820 (2000).

[12] J. Linnros, N. Lalic, A. Galeckas, and V. Grivickas, J. Appl. Phys. **86**, 6128 (1999).

Appendix A

Nederlandse samenvatting

Silicium (Si) is het meest voorkomende halfgeleider materiaal op aarde en heeft mede hierdoor het grootste aandeel in de electronische industrie. Helaas is het vermogen van Si om licht te absorberen en te emitteren slecht door zijn indirecte bandgap. Dit vormt een groot obstakel voor de toepassing van Si in photonische systemen. Si nanokristallen (NCs) bieden een mogelijke uitkomst. Door het quantum confinement effect dat optreedt in deze structuren wordt de indirecte bandgap weliswaar groter en door de relaxatie van de momentum conservatie regel wordt de efficiency om licht te emitteren sterk vergroot als de NCs kleiner worden. Dit verslag beschrijft onderzoek naar een nieuw phenomeen in Si NCs, veroorzaakt door quantum confinement. Er wordt aangetoond dat in tegenstelling tot de indirecte bandgap de directe bandgap mogelijk juist kleiner wordt. Er is al aangetoond dat voor kleinere NCs een directe recombinatie waarschijnlijker wordt. Samen met het verkleinen van de directe bandgap baant dit een weg voor Si in photonische en photovoltaische systemen.